J Nanostruct 16(4): 5411-5419, Autumn 2026

RESEARCH PAPER

Influence of CuO Nanoparticles Additive on Performance of CuO/PVC Nanocomposite Thin Films Coatings

Suhair G. Hussein [1] *, *Farah H. Rashid* [2]

[1] *Mechanical Engineering Department, University of Baghdad, Iraq*

[2] *Collage of Biomedical Instrumentation Engineering, University of Technology, Iraq*

ARTICLE INFO

Article History:
Received 10 June 2026
Accepted 17 September 2026
Published 01 October 2026

Keywords:
Copper oxide (CuO)
Dip-coating
Hydrothermal synthesis
Nanocomposite thin films
Polyvinyl chloride (PVC)
X-ray diffraction (XRD)

ABSTRACT

Metal oxides are one of the most versatile classes of materials due to the variety of their structural, optical, electrical and catalytic properties. Of these, copper oxide (CuO) has been the subject of much research due to its possible applications in solar energy conversion, optoelectronic devices, photocatalysis, and antimicrobial products. In this study, CuO/PVC nanocomposite thin films were fabricated by the incorporation of the hydrothermally synthesized CuO nanocrystals in a polyvinyl chloride (PVC) matrix. Films were prepared by the dip-coating technique from a homogeneous solution of PVC in a colloidal solution of CuO nanoparticles onto glass substrates. The structural properties of the nanocomposite films were studied by X-ray diffraction (XRD), and the results demonstrated the incorporation of the monoclinic CuO nanocrystals into the mainly amorphous PVC matrix. The diffraction peaks showed good crystallinity of the CuO phase, and the average crystallite size was calculated to be about 15 nm by Debye–Scherrer equation. The formation of the nanocomposite was further confirmed by Fourier transform infrared (FTIR) spectroscopy with the characteristic Cu–O vibration band as well as the absorption bands of the PVC matrix. UV–Visible spectroscopy has been used to check the optical properties. The characteristic absorption band centered at ~372 nm was observed in the absorption spectrum, which confirmed the optical response of embedded CuO nanoparticles in the polymer matrix. The results obtained prove the successful preparation of CuO/PVC nanocomposite thin films with suitable structure and optical properties, which can be used in optoelectronic functional coatings applications.

How to cite this article
Hussein S., Rashid F. Influence of CuO Nanoparticles Additive on Performance of CuO/PVC Nanocomposite Thin Films Coatings. J Nanostruct, 2026; 16(4):5411-5419. DOI: 10.22052/JNS.2026.04.075

INTRODUCTION

The global community has focused on materials with appropriate and sustainable qualities in recent years. A range of doping materials can be used to improve attributes. The most important elements affecting these characteristics are their nature and the synthesis process. Researchers are guided by targeted applications and cost when selecting materials and technologies to create the intended gadgets. Researchers are becoming more interested in polymers, especially hybrid composites (organic-inorganic), due to their widespread usage in several industries. Higher physical and chemical stability can be achieved by

* *Corresponding Author Email: suhair.g.hussein@coeng.uobaghdad.edu.iq*

incorporating metal oxides, such as ZnO, TiO_2, SnO_2, and other semiconductors, into organic matrices [1-4]. These nanocomposites can have organic polymers as matrix and inorganic nanoparticles as fillers. Organic polymers as matrix and inorganic nanoparticles as fillers can provide the These nanocomposites demonstrate the benefits of combining the flexibility and processability of polymers with the beneficial qualities of metal oxides. resulting in nanocomposites with superior mechanical, optical, and electrical qualities [5]. The filler is represented by CuO, while the host matrix is represented by the polymer polyvinyl chloride. Copper (II) oxide CuO is one of the most significant metal oxides. It is the most basic member of the copper compound family and possesses a number of crucial physical characteristics, including non-toxicity, electronic correlation, and superconductivity at high temperatures. Because of the comparatively low band gap in its crystal structure, it displays intriguing photovoltaic and photoconductive capabilities [6]. Conversely, PVC has translucent thin sheets and is inexpensive. Therefore, in order to enhance the structural and optical characteristics of the CuO-PVC nanocomposite thin films, which are created by directly adding nanoscale CuO semiconductor particles to PVC polymer and coated on glass substrates using a dip-coating approach. XRD and FT-IR spectroscopy were used for structural analysis, while photoluminescence and UV-visible optical absorption were used to emphasize the optical characteristics [7].

MATERIALS AND METHODS

Experimental work of synthesis of CuO nanoparticles

The analytic-grade chemical reagents utilized in this study (Fig. 1) were not further purified during the whole experiment. As a solvent, we employed distilled water, sodium hydroxide (NaOH), and copper sulfate pentahydrate (CuSO4-5H2O). Typically, a homogenous blue solution was produced by dissolving 0.5 g of CuSO4-5H2O in 40 mL of distilled water while stirring continuously. Next, 5 milliliters of sodium hydroxide (1M) aqueous solution were added. The mixture was then magnetically agitated for half an hour. After a blue precipitate formed, the mixture was put into a stainless autoclave lined with Teflon. After that, the autoclave is placed in an oven and maintained at 200°C for two hours. The autoclave was then allowed to spontaneously cool to ambient temperature. The black precipitate was gathered, repeatedly cleaned with distilled water, and then allowed to dry naturally [8].

Preparation of CuO – PVC nanocomposite

The CuO-PVC nanocomposite was created

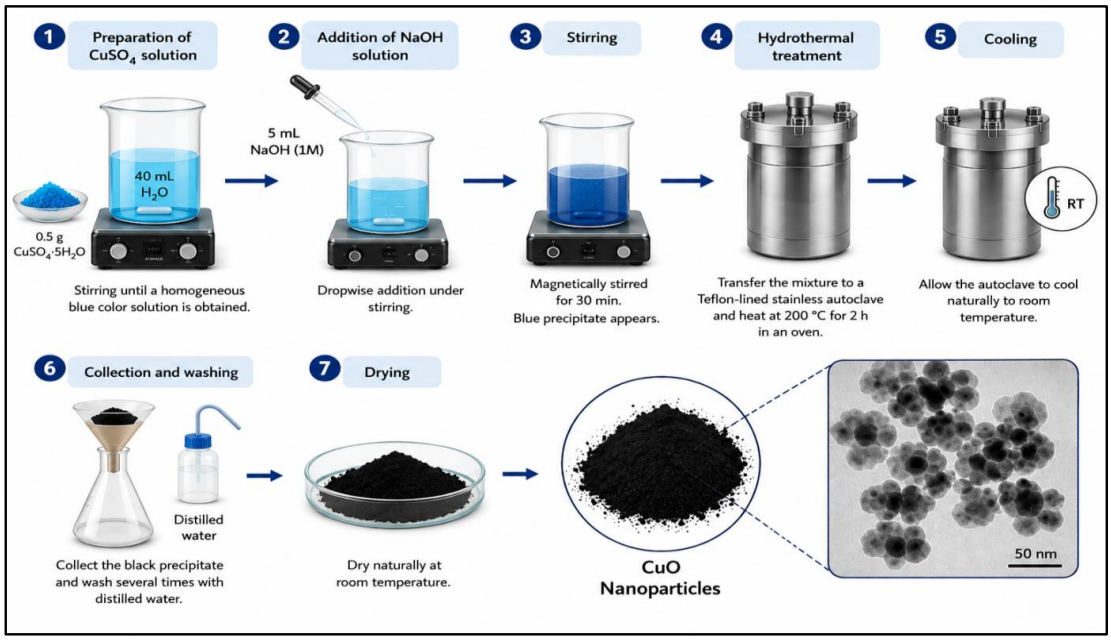

Fig. 1. Synthesis of CuO nanoparticles.

by embedding the CuO nanoparticles in the polyvinyl chloride (PVC) polymer matrix. The following process was used to create the CuO-PVC nanocomposite films. Using a magnetic stirrer, 0.5 g of PVC was dissolved in 10 mL of tetrahydrofuran (THF) as a solvent. The PVC-THF mixture was supplemented with copper oxide (CuO) nanoparticles at a ratio of PVC/CuO=10. To get a homogenous solution, the mixture was agitated at room temperature. The substrate glass slides were carefully rinsed with distilled water after being cleaned with ethanol. As shown in Fig. 2, thin films were applied to substrates using the dip-coating approach [9].

RESULTS AND DISCUSSION

XRD analysis of CuO nanoparticles

The X-ray diffraction (XRD) pattern Fig. 3 shows multiple low-intensity peaks at higher diffraction angles, together with a prominent diffraction peak at about 2θ = 35.5°. A favored crystallographic orientation is indicated by the main peak's high intensity, which implies that a significant portion of the crystallites are oriented along a certain crystallographic plane. Furthermore, a low concentration of crystal flaws and good crystallinity are indicated by the primary diffraction peak's small breadth. Diffraction from additional crystallographic planes with lower relative strengths is represented by the weak secondary peaks. Overall, the diffraction pattern demonstrates that the sample is crystalline. However, comparing the diffraction peak positions with a common reference database (JCPDS/ICDD) is necessary for definitive phase identification. [10,11].

X-ray diffraction (XRD) pattern for CuO/PVC nanocomposite

The X-ray diffraction (XRD) pattern of the CuO/PVC nanocomposite Fig. 4 exhibits a combination of a broad diffraction halo and several sharp diffraction peaks, indicating the coexistence of an amorphous polymer matrix and a crystalline inorganic phase. The wide background of the diffraction pattern is observed due to the dominant amorphous character of PVC matrix and sharp diffraction peaks are of crystalline CuO nanoparticles embedded in the polymer. [12]. The strongest diffraction peaks appear at about 2θ = 35.5° and 38.7° which are typical diffraction angles for the monoclinic structure of CuO, with other diffraction angles at higher 2θ values attributed to other crystallographic planes of CuO. The

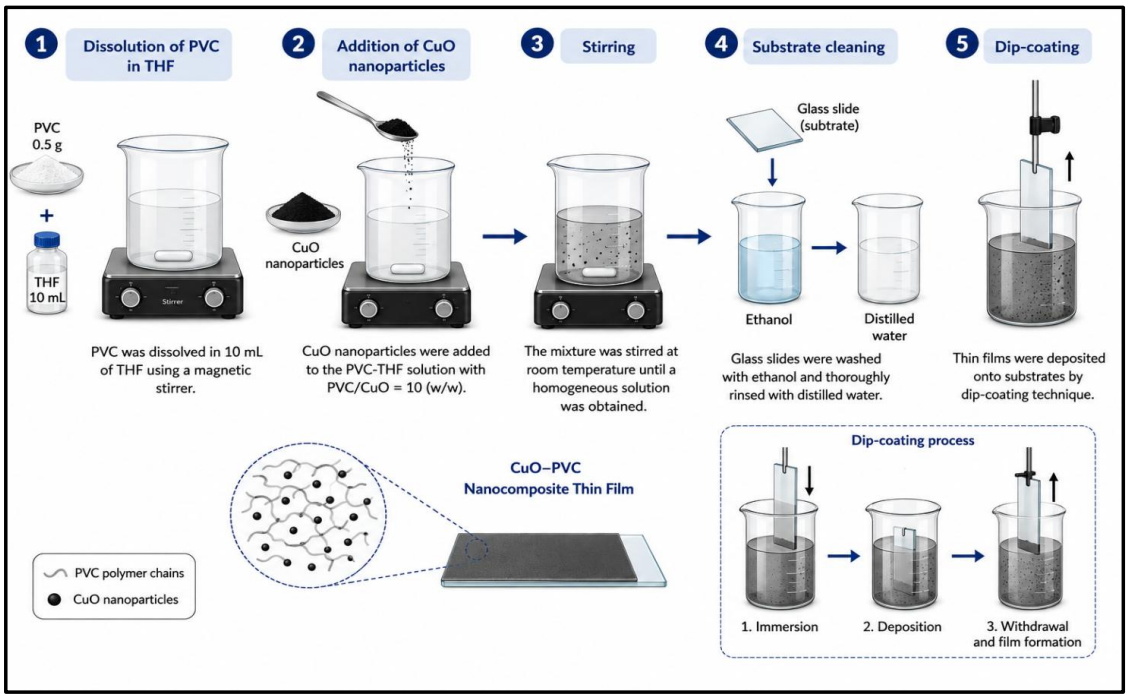

Fig. 2. Preparation of CuO –PVC nanocomposite.

characteristic diffraction peaks of CuO are retained to show that the crystallographic structure of CuO does not change upon incorporation into the PVC matrix. In addition, no additional diffraction peaks of secondary crystalline phase can be observed, indicating that there is no detectable impurity phase formed during the preparation process. The broad amorphous nature of PVC and the presence of the CuO diffraction peaks confirm the successful incorporation and uniform dispersion of CuO nanoparticles in the polymer matrix. The sharpness and relatively high intensity of the CuO diffraction peaks also indicate good crystallinity of the nanoparticles, which is expected to enhance

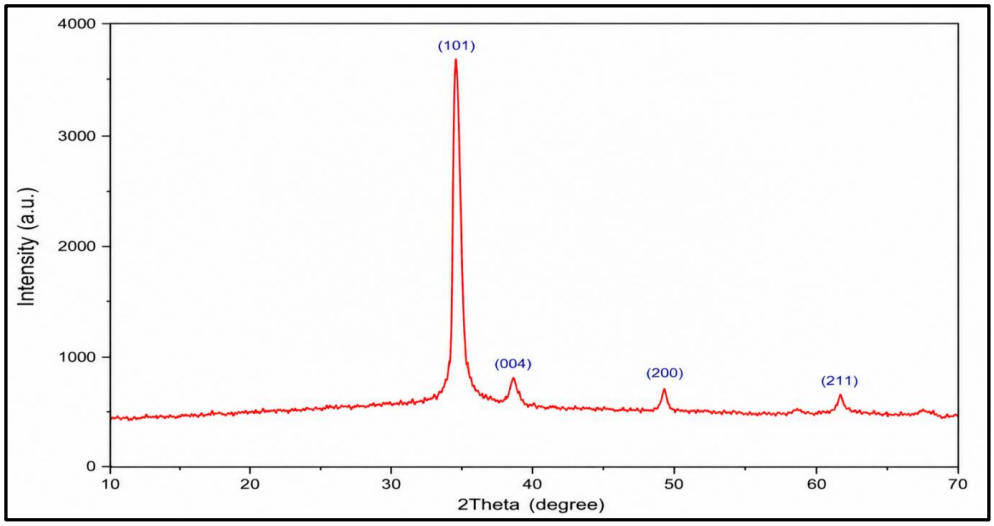

Fig. 3. The X-ray diffraction for CuO NPs.

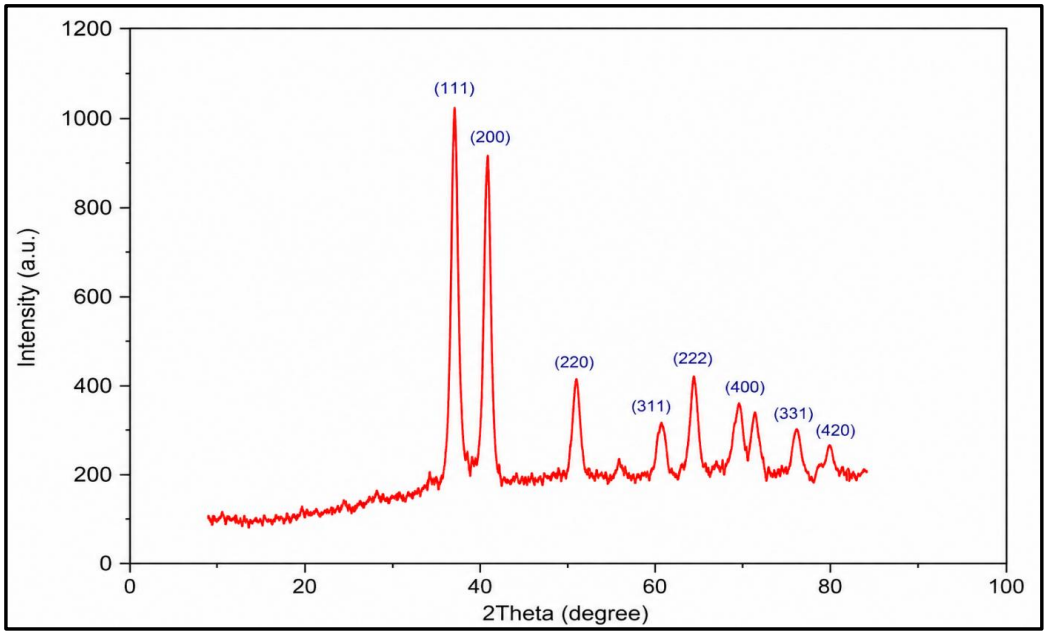

Fig. 4. XRD for CuO/PVC nanocomposite.

[13,14].

FT-IR for CuO/PVC nanocomposite

One technique to highlight the finer surface information is FTIR spectroscopy in attenuated total reflection (ATR) mode. CuO-PVC nanocomposite overlapped FTIR spectra. The CuO-PVC nanocomposite exhibits comparable bands between -600 and 5000 cm^{-1}. Pure PVC is characterized by the bands seen at 611, 1064, 1250, and 2904 cm^{-1} [15]. The asymmetric *C*3-H stretching frequencies of alkyl groups are represented by the band at 2990 cm^{-1} [16]. There is a band at 3670 cm−1 for the free OH functional group. Regarding the CuO powder, the bands at 480 and 610 cm^{-1} correspond to the CuO nanoparticles integrated into the PVC. The band at 480 cm^{-1} is clearly visible on the CuO-PVC nanocomposite spectrum Fig. 5, whereas the band at 610 cm^{-1}. The band at 480 cm^{-1} is clearly visible on the CuO-PVC nanocomposite spectrum (Fig. 5), however the band at 610 cm^{-1} is superposed with the PVC band. When compared to pure PVC, the CuO-PVC nanocomposite had no band shift, indicating a very weak or nonexistent chemical bonding relationship between the CuO nanoparticles and pure PVC [17].

UV-Visible optical absorption analysis

The UV–Vis transmittance spectra of pure CuO nanoparticles and the CuO/PVC nanocomposite thin film are presented in Figs. 6 and 7, respectively. As shown in Fig. 6, the pure CuO sample exhibits relatively low transmittance over the investigated wavelength range, increasing gradually from the ultraviolet to the near-infrared region. This behavior is attributed to the strong optical absorption of CuO, which originates from its narrow band gap and high density of electronic states. In contrast, the CuO/PVC nanocomposite thin film Fig. 7 exhibits a pronounced increase in transmittance, reaching approximately 85–86% above 300 nm and remaining nearly constant throughout the visible and near-infrared regions. [18]. This substantial increase in optical transmittance upon the addition of the CuO nanoparticles in the PVC matrix is primarily attributed to the optical transparency of PVC, and the dispersion of CuO nanocrystals in the amorphous PVC matrix, which results in a uniform distribution of optical properties. Moreover, the sudden rise of transmittance in the UV range is the fundamental absorption edge of the nanocomposite material, and the practically constant transmittance in the visible range suggests that optical losses are low and that the quality of the film is good. The results indicate that these thin films are highly transparent with the incorporation of CuO nanocrystals and possess the same optical response as CuO, thus enabling the

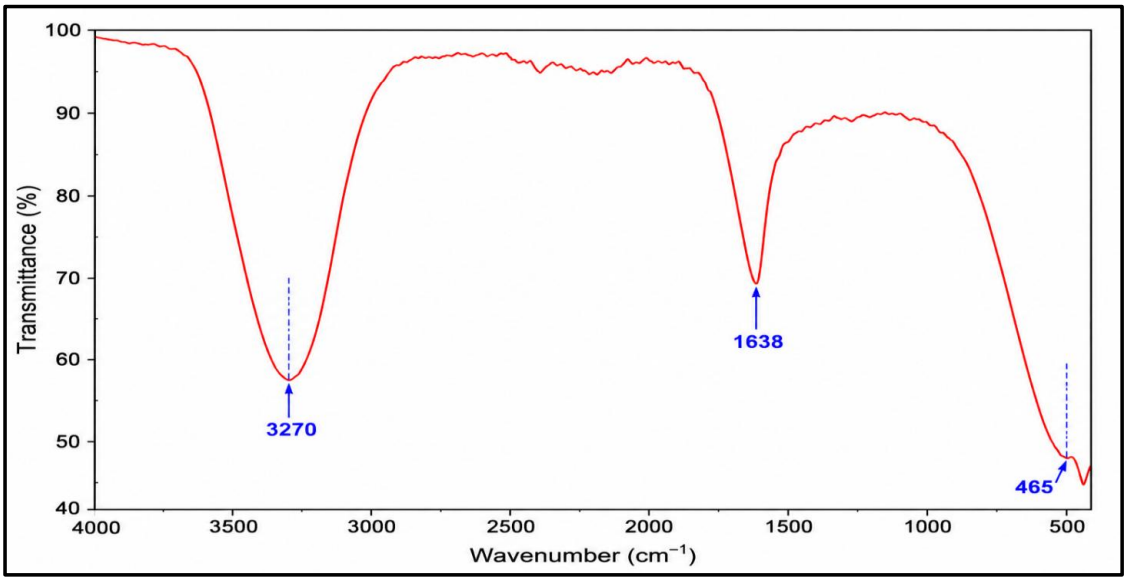

Fig. 5. FT-IR for CuO/PVC nanocomposite.

use of CuO/PVC nanocomposites in transparent coating and optical electronic applications [19].

Gas-Sensing Behavior of CuO/PVC Nanocomposites

The gas-sensing behavior of the fabricated CuO/PVC nanocomposite films was investigated at a fixed gas concentration of 5 ppm. The results demonstrate a clear improvement in the gas response with increasing CuO content. The gas response of the CuO/PVC composite containing 3 wt% CuO was approximately 45, whereas the response increased to about 66 when the CuO concentration was increased to 5 wt%. This corresponds to an enhancement of approximately 46.7% in the gas response. As shown in Figs. 8 and 9, the increase in CuO loading significantly

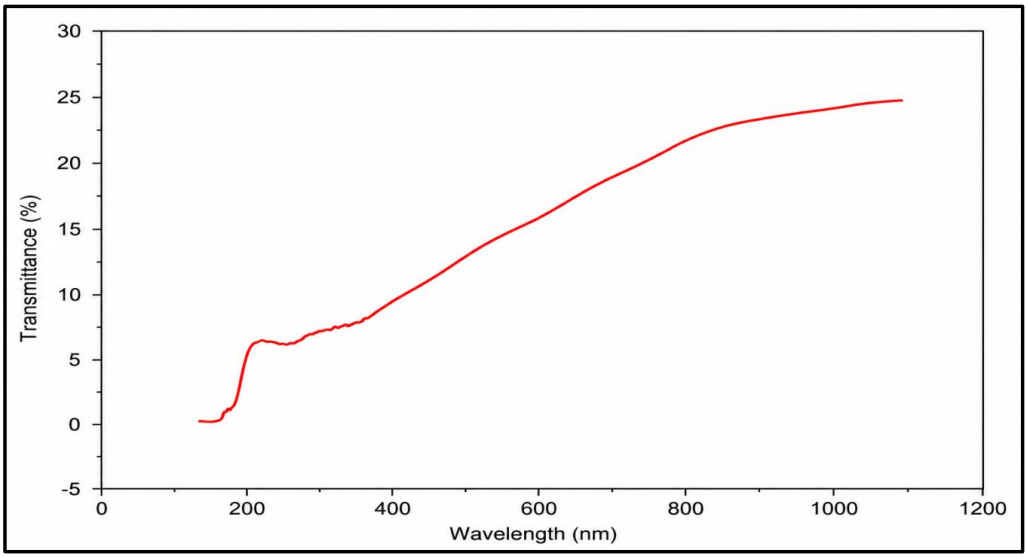

Fig. 6. The UV–Vis transmittance spectra of pure CuO nanoparticles.

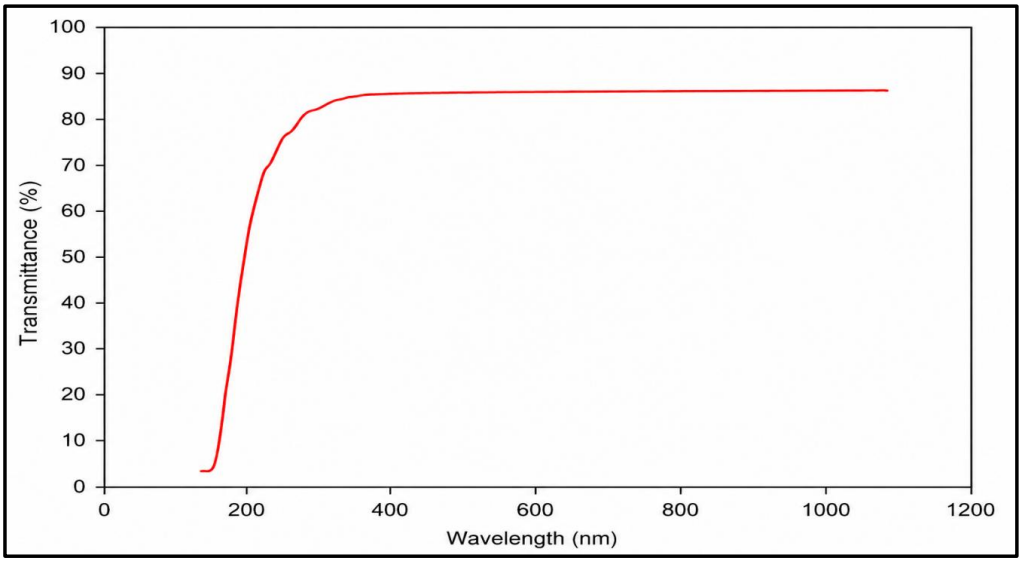

Fig. 7. The UV–Vis transmittance spectra of CuO/PVC nanocomposite.

improves the sensing performance of the CuO/PVC nanocomposite films.

The observed enhancement in gas response can be mainly attributed to the electrical and surface characteristics of CuO within the PVC matrix. CuO is a p-type semiconducting metal oxide with a narrow band gap, whereas PVC is an electrically insulating polymer. At the relatively low CuO concentration of 3 wt%, the CuO nanoparticles are distributed within the PVC matrix, but the insulating polymer phase can limit the formation of efficient charge-transport pathways between neighboring CuO particles. When the CuO concentration is increased to 5 wt%, the distance between adjacent CuO nanoparticles decreases and the probability of particle-to-particle contact increases. Consequently, a more interconnected CuO network can be established within the PVC matrix, facilitating charge transport and producing a stronger electrical response during gas exposure.

In addition to improving electrical connectivity, increasing the CuO content provides a larger active

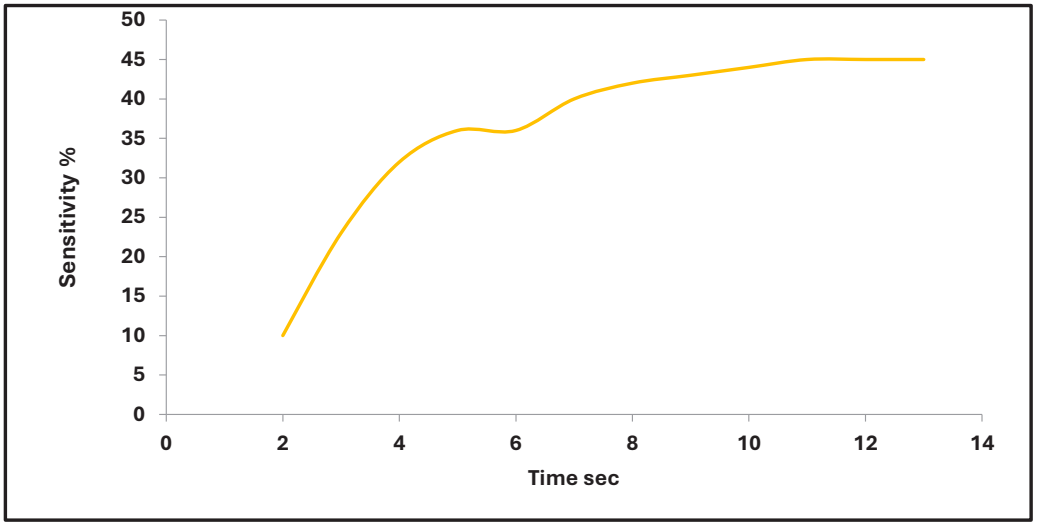

Fig. 8. Sensitivity of CuO/PVC films for NO_2 gas.

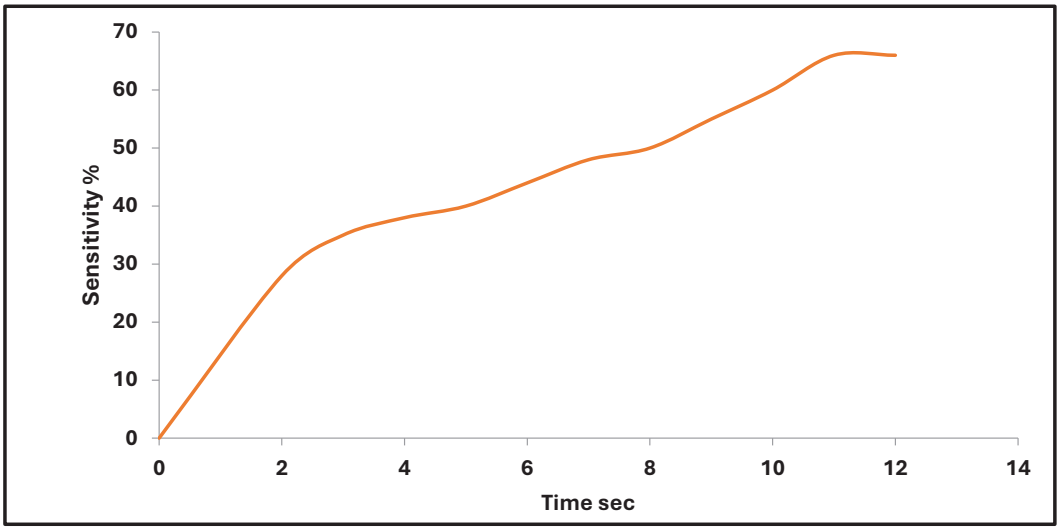

Fig. 9. Sensitivity of CuO/PVC films for NO_2 gas.

surface area for interaction with gas molecules. Metal-oxide semiconductor gas sensors generally depend strongly on surface adsorption and surface reactions because adsorbed gas species can modify the electrical conductivity of the sensing material. The surface of CuO contains active sites that can interact with gas molecules through adsorption processes. Gas molecules adsorbed on the CuO surface can exchange charge with the semiconductor and modify the concentration of charge carriers, resulting in changes in the electrical resistance of the sensing film [5,7]. Since CuO constitutes the primary semiconducting component of the composite, these gas-induced electrical changes become more pronounced as the CuO content increases.

Another important factor is the CuO–PVC interfacial region. The incorporation of CuO nanoparticles into the PVC matrix produces numerous interfaces where charge-transfer processes can be affected by the adsorption of gas molecules. Increasing the CuO concentration from 3 wt% to 5 wt% increases the number of CuO nanoparticles and consequently increases the number of CuO–CuO and CuO–PVC interfaces. Such interfaces can influence charge transport and provide additional sites for interaction between the sensing layer and the surrounding gas molecules. Therefore, the improvement in gas response is not simply related to the increased amount of CuO, but also to the formation of a more effective interconnected CuO network and the increased number of gas-interaction sites.

Because the gas concentration was maintained at 5 ppm for both compositions, the comparison between the responses of approximately 45 and 66 provides a direct indication of the effect of CuO loading. Assuming that the measurement conditions, film thickness, operating temperature, and electrical measurement procedure were kept constant, the increase in gas response can reasonably be attributed to increasing the CuO content from 3 wt% to 5 wt%. The higher response obtained for the 5 wt% CuO/PVC composite indicates that this composition provides more favorable conditions for gas adsorption and gas-induced modulation of charge transport. the results demonstrate that increasing the CuO concentration from 3 wt% to 5 wt% enhances the gas-sensing performance of the CuO/PVC nanocomposite films. The improvement can be attributed to the increased number of active CuO surface sites, enhanced gas adsorption, improved interparticle connectivity, and stronger modulation of charge transport within the CuO/PVC structure. These findings highlight the important role of CuO loading in controlling the gas-sensing properties of PVC-based metal-oxide nanocomposite films.

CONCLUSION

CuO with an average diameter of 10–23 nm has been created in thin film form using the dip-coating method and distributed throughout a PVC matrix. XRD, FT-IR, and UV-VIS-NIR absorption were used to examine the structural and optical characteristics of the as-prepared composite. The XRD analysis revealed the monoclinic crystalline phase of CuO. The results of the XRD investigation on the production of the CuO-PVC nanocomposite are confirmed by the FT-IR spectroscopy analysis, which revealed the presence of Cu–O vibration modes. An intermediate absorption edge between that of pure PVC and that of the semiconductor CuO is revealed by the optical measurement results.

CONFLICT OF INTEREST

The authors declare that there is no conflict of interests regarding the publication of this manuscript.

REFERENCES

1. Fung MK, Wong KK, Chen XY, Chan YF, Ng AMC, Djurišić AB, et al. Indium oxide, tin oxide and indium tin oxide nanostructure growth by vapor deposition. Current Applied Physics. 2012;12(3):697-706.
2. Bender M, Katsarakis N, Gagaoudakis E, Hourdakis E, Douloufakis E, Cimalla V, et al. Dependence of the photoreduction and oxidation behavior of indium oxide films on substrate temperature and film thickness. J Appl Phys. 2001;90(10):5382-5387.
3. Berry L, Brunet J, Varenne C, Mazet L, Pauly A, Wierzbowska K. NO_2 gas sensing studies: Impact of geometrical and physical characteristics of ohmic contacts on n-InP epitaxial sensitive layer. Materials Science and Engineering: C. 2007;27(4):654-658.
4. Mosaddeq-ur-Rahman M, Yu G, Soga T, Jimbo T, Ebisu H, Umeno M. Refractive index and degree of inhomogeneity of nanocrystalline TiO_2 thin films: Effects of substrate and annealing temperature. J Appl Phys. 2000;88(8):4634-4641.
5. Gnanam S, Rajendran V. Preparation of Cd-doped SnO_2 nanoparticles by sol–gel route and their optical properties. J Sol-Gel Sci Technol. 2010;56(2):128-133.
6. Basu S, Basu PK. Nanocrystalline Metal Oxides for Methane Sensors: Role of Noble Metals. Journal of Sensors. 2009;2009(1).
7. Beshkov G, Kolentsov K, Yourukova L, Rachkova A, Mateeva D. Influence of rapid thermal annealing on the properties of SnO_2 thin films. Materials Science and Engineering: B.

1995;30(1):1-5.
8. Mosadegh Sedghi S, Mortazavi Y, Khodadadi A. Low temperature CO and CH4 dual selective gas sensor using SnO2 quantum dots prepared by sonochemical method. Sensors Actuators B: Chem. 2010;145(1):7-12.
9. Sun XW, Wang LD, Kwok HS. Improved ITO thin films with a thin ZnO buffer layer by sputtering. Thin Solid Films. 2000;360(1-2):75-81.
10. Anvarifard MK, Ramezani Z, Ghoreishi SA. Enabling Oxygen Gas Detection via Graphene-Nanoribbon FET (GNRFET) on 6H-SiC Substrate Utilizing a Catalytic Gate Electrode. Silicon. 2024;16(6):2651-2657.
11. Kong XY, Wang ZL. Structures of indium oxide nanobelts. Solid State Commun. 2003;128(1):1-4.
12. Staudinger U, Janke A, Simon F, Jakisch L, Bittrich E, Formanek P, et al. MWCNT Localization and Electrical Percolation in Thin Films of Semifluorinated PMMA Block Copolymers. Polymers. 2025;17(9):1271.
13. Eranna G, Joshi BC, Runthala DP, Gupta RP. Oxide Materials for Development of Integrated Gas Sensors—A Comprehensive Review. Crit Rev Solid State Mater Sci. 2004;29(3-4):111-188.
14. Steffes H, Imawan C, Solzbacher F, Obermeier E. Enhancement of NO_2 sensing properties of In2O3-based thin films using an Au or Ti surface modification. Sensors Actuators B: Chem. 2001;78(1-3):106-112.
15. Fan JCC, Goodenough JB. X-ray photoemission spectroscopy studies of Sn-doped indium-oxide films. J Appl Phys. 1977;48(8):3524-3531.
16. Qiao Z, Latz R, Mergel D. Thickness dependence of In_2O_3:Sn film growth. Thin Solid Films. 2004;466(1-2):250-258.
17. Vaishnav VS, Patel PD, Patel NG. Indium Tin Oxide thin film gas sensors for detection of ethanol vapours. Thin Solid Films. 2005;490(1):94-100.
18. Farhana N. Bio-Inspired Swarm-Transformer Hybrid Algorithm for HighPrecision Nanomaterial Design and Experimental Validation in Biomedical Applications. Ci-STEM Journal of Advanced Materials and Computing. 2026;01(01):09-16.
19. Makhija KK, Ray A, Patel RM, Trivedi UB, Kapse HN. Indium oxide thin film based ammonia gas and ethanol vapour sensor. Bull Mater Sci. 2005;28(1):9-17.